

Video Surveillance of Highway Traffic Events by Deep Learning Architectures [★]

Matteo Tiezzi¹, Stefano Melacci¹, Marco Maggini¹, and Angelo Frosini²

¹ Department of Information Engineering and Mathematics, University of Siena

<http://sailab.diism.unisi.it>
{mtiezzi,mela,maggini}@diism.unisi.it

² IsTech s.r.l., Pistoia, Italy
a.frosini@istech.it

Abstract. In this paper we describe a video surveillance system able to detect traffic events in videos acquired by fixed videocameras on highways. The events of interest consist in a specific sequence of situations that occur in the video, as for instance a vehicle stopping on the emergency lane. Hence, the detection of these events requires to analyze a temporal sequence in the video stream. We compare different approaches that exploit architectures based on Recurrent Neural Networks (RNNs) and Convolutional Neural Networks (CNNs). A first approach extracts vectors of features, mostly related to motion, from each video frame and exploits a RNN fed with the resulting sequence of vectors. The other approaches are based directly on the sequence of frames, that are eventually enriched with pixel-wise motion information. The obtained stream is processed by an architecture that stacks a CNN and a RNN, and we also investigate a transfer-learning-based model. The results are very promising and the best architecture will be tested online in real operative conditions.

Keywords: Convolutional Neural Networks, Recurrent Neural Networks, Deep Learning, Video Surveillance, Highway Traffic

1 Introduction

The progressive growth of the number of vehicles, that nowadays are traveling on roads and highways, has created high interest in the research areas related to the development of techniques needed in automatic instruments for traffic monitoring. These systems are generically referred to as Intelligent Transportation Systems (ITSs). Basic tasks, that are to be accomplished by ITSs, are the identification of vehicles and of their behaviour from video streams, captured by surveillance cameras installed along the road connections. The automatic detection of specific events happening in the traffic flow, such as accidents, dangerous

[★] This is a post-peer-review, pre-copyedit version of an article published in LNCS, volume 11141. The final authenticated version is available online at: https://doi.org/10.1007/978-3-030-01424-7_57

driving, and traffic congestions, has become an indispensable functionality of ITSs since it is impractical to employ human operators both for the number of control points and the need of a continuous attention. Automatic notifications guarantee an immediate response to exceptional events such as car crashes or wrong-way driving. At the same time, the estimation of road congestion allows us to notify drivers and to provide information for optimizing the itineraries computed by navigation devices. This field of research began to be particularly active in the '80, with projects funded by governments, industries and universities, in Europe (PROMETHEUS [12]), Japan (RACS [10]) and the USA (IVHS [1]). These studies included autonomous cars, inter-vehicle communication systems [7], surveillance and monitoring of traffic events [8,3].

Among the general ITSs, the Advanced Traffic Management Systems (ATMS) are aimed at exploiting all the information coming from cameras, sensors and other instruments, positioned along highways and main routes, to provide an analysis of the current state of traffic and to respond in real time to specific conditions. Signals from all devices are gathered at a central Transportation Management Center that must implement technologies capable of analyzing the huge amounts of data coming from all the sensors and cameras.

In this context, Machine Learning provides tools to tackle many problems faced in the design of the ATMS modules. In particular, Deep Neural Network architectures are able to yield state-of-the-art performances in many computer vision tasks [4] and are currently applied in real systems, such those for autonomous driving [2]. Hence, most of current video surveillance modules are based on deep learning techniques, that allow us to tune the system just by providing enough examples of the objects or events of interest [13]. The wide use of these approaches has also been driven by the availability of pre-trained architectures for computer vision tasks that can be adapted to new problems by transfer learning [9].

The objective of this work is the creation of an instrument capable to perform a real time/on-line analysis of data coming from cameras, in order to detect automatically significant events occurring in the traffic flow. We analyze the results obtained by different approaches on real videos of traffic on highways. In particular we compare an approach based on precomputed motion features processed by a Recurrent Neural Network (RNN) with a technique exploiting the original video augmented by channels to encode the optical flow. The latter is based on an architecture composed by a Convolutional Neural Network (CNN), processing each input frame, stacked with a RNN. We consider both the cases in which the CNN is learned from our traffic videos and when it is a pre-trained CNN in a transfer learning scheme.

The paper is organized as follows. The next Section describes the considered problem, while our dataset and the feature representation are described in Section 2. In Section 4 we introduce the selected deep neural network architectures, while Section 5 reports the results. Finally, Section 6 concludes the paper.

2 Video Surveillance of Highway Traffic

We focus on a system that processes videos acquired by fixed cameras on highways. Cameras can be positioned in very different environments (e.g. tunnels or outdoor) and can have many different settings for the point of view (e.g. long or short range, wide or narrow span). Moreover, videos are captured in different environmental and weather conditions (daylight, night, fog, rain, etc.). The system is expected to detect specific events of interest happening in the scene for a variable time interval. In particular, we consider four different classes of events, collected in the set \mathcal{E} (see Fig. 1):

- **Stationary vehicle**, a vehicle stops inside the field of the camera;
- **Departing vehicle**, a vehicle, previously stationary, departs from his position;
- **Wrong-way vehicle**, a vehicle moves in the wrong direction;
- **Car crash**, accident involving one or more vehicles.



Fig. 1: The four different classes of events. (a) Stationary. (b) Departing. (c) Wrong-way. (d) Car crash.

As already stated, all the videos are captured by cameras positioned in different places and settings on highways, including tunnels and high-speed stretches. This fact entails several issues that can deteriorate the prediction performances. For instance, cameras are exposed to all kind of weather conditions, including fog, rain or strong wind. Another relevant problem is due to variations in brightness caused by tunnel lamps activation, clouds passing by, and sun movement (see Fig. 2 for examples).

3 Data Description and Representation

Video surveillance cameras provide a continuous stream of a given view of the highway along the direction of the traffic flow. Due to the nature of the events we are trying to detect, it was difficult to collect a large dataset of examples³. For instance, some events like wrong-way driving are quite rare.

³ The dataset was collected thanks to IsTech srl and was based only on a limited number of fixed cameras.

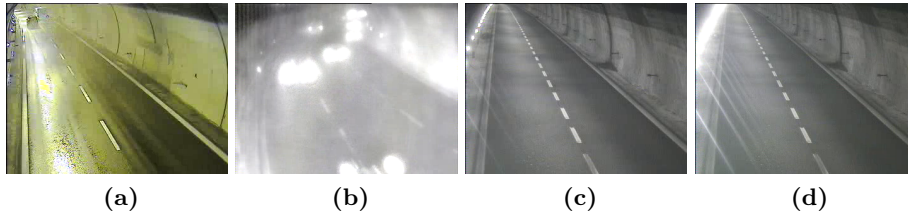


Fig. 2: Conditions causing difficulties in video analysis. (a) Rain. (b) Fog. (c)-(d) Brightness variation, before and after.

Videos were captured in colors in two standard resolutions (352×288 and 640×320 pixels, depending on the camera type) at 25 frames per second. In some cases the videocamera includes the lanes in both directions in its field. Hence, in order to remove potential sources of misleading information (for instance, related to wrong-way vehicles) each frame is masked with a template that keeps only the portion related to the lanes to be considered (see Fig. 4).

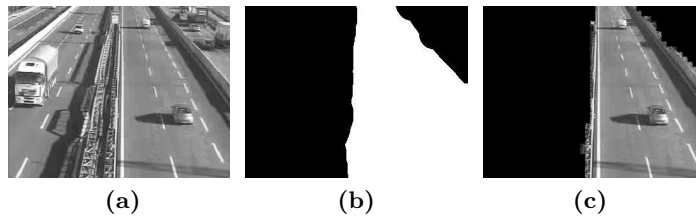


Fig. 3: (a) Original frame. (b) Mask. (c) Masked frame.

We down-sampled the available videos at 2 frames per second, and extracted clips of 125 frames (1 minute), containing instances of the events \mathcal{E} listed in Section 2, as well as clips with normal traffic conditions. To avoid artificial regularities that may hinder the generalization, the clips are generated such that events can happen in every instant inside the 125 frame interval, apart from the very beginning or ending. The statistics of the available dataset used in training and testing are reported in Tab. 1. The optical flow algorithm⁴ was exploited

Table 1: Statistics of the dataset used in the paper.

	No Event	Stationary	Departing	Wrong-way	Car crash	Total
# Clips	281	111	56	131	16	595

to compute the motion field for each input frame. Each frame was resized and cropped to 160×120 pixels. We represented the input frames in three different ways, using *i.* pre-designed motion features, *ii.* appearance, or *iii.* appearance and motion, as described in the following.

Representation by motion features. Due to the effect of perspective, moving objects closer to the camera position have an apparent motion larger than distant objects. Therefore, we decided to split each frame into four horizontal stripes as shown in Fig. 4a. For each stripe the directions and modules of the optical flow are quantized, building a histogram of the distribution of the motion vectors. In the implementation we considered 32 bins based on 8 directions and 4 levels for the module (Figure 4b). This scheme yields 128 values (32 bins for each stripe) collected into a vector for each frame. In order to provide evidence for stationary vehicles, we computed an additional feature for each stripe as follows. We applied and manually tuned a Background Subtraction [6] method to extract the pixels not belonging to the static background of the video (see Figure 4c). The additional feature per stripe is the count of non-background pixels having null motion. Hence, each frame is represented by a vector of 132 entries.

Representations by appearance and motion. The appearance-based representation consists of the raw frame converted to grayscale to reduce the image variability. Another representation is obtained by adding two additional channels for each frame corresponding to the horizontal and vertical components of the motion field provided by the optical flow, leading to a $160 \times 120 \times 3$ tensor.

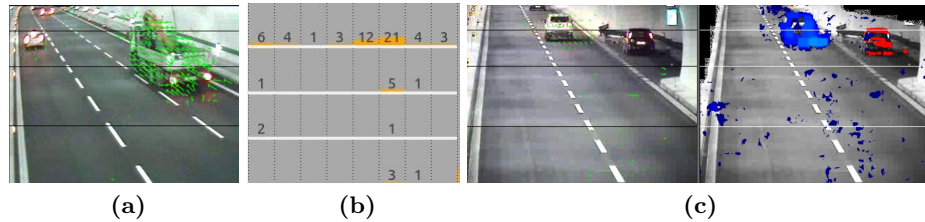


Fig. 4: (a) Motion vectors, frame partitioned into 4 stripes. (b) Histogram computed in one stripe. (c) Background subtraction (original frame on the left, estimated not-background objects on the right).

4 Deep Architectures

We are given a video stream \mathcal{V} that produces frames at each time instant t . At a certain $t > 0$, we have access to the sequence of frames up to time t , that we

⁴ We used the default implementation in the OpenCV library <https://opencv.org/>, based on the Farneback’s algorithm.

indicate with $\mathcal{S}_t = \{\mathcal{I}_i, i = 1, \dots, t\}$, where \mathcal{I}_i is the i -th frame of the sequence. We implemented multiple deep architectures that learn to predict the set of events Y_t that characterize frame \mathcal{I}_t , given the sequence \mathcal{S}_t . Formally, if $f(\cdot)$ is a generic deep neural network, we have

$$Y_t = f(t|\mathcal{S}_t) ,$$

where $Y_t = \{y_{t,h}, h = 1, \dots, |\mathcal{E}|\}$ is a set of predictions of the considered events \mathcal{E} (in this work, $|\mathcal{E}| = 4$). In particular, $y_{t,h} \in \{0, 1\}$, where $y_{t,h} = 1$ means that the h -th event is predicted at time t .

Before being processed by the network, each frame \mathcal{I}_i is converted into one of the three representations that we described in Section 3, generically indicated here with r_i ,

$$r_i = \text{frame_representation}(\mathcal{I}_i) . \quad (1)$$

Our deep architecture $f(\cdot)$ is then composed of four computational stages, and each of them projects its input into a new latent representation. Stages consist of a feature extraction module **feature_extraction**(\cdot), a sequence representation module **sequence_representation**(\cdot), a prediction layer **predictor**(\cdot), and a decision function **decision**(\cdot) that outputs Y_t ,

$$q_t = \text{feature_extraction}(r_t) \quad (2)$$

$$s_t = \text{sequence_representation}(q_t, s_{t-1}) \quad (3)$$

$$p_t = \text{predictor}(s_t) \quad (4)$$

$$Y_t = \text{decision}(p_t) . \quad (5)$$

Eq. (2) is responsible of extracting features from r_t , building a new representation q_t of the current frame. We implemented multiple extractors, in function of the method selected to produce r_t (we postpone their description). Eq. (3) encodes the sequence of frames observed so far. The sequence representation s_t is computed by updating the previous representation s_{t-1} with the current input r_t . This is implemented with a Recurrent Neural Network (RNN), where s is the hidden state of the RNN. In particular, we used a Long Short Term Memory RNN (LSTM) [5], and we also experienced multiple layers of recurrence (2 layers). Eq. (4) is a fully connected layer with sigmoidal activation units, that computes the event prediction scores $p_t \in [0, 1]^{|\mathcal{E}|}$. We indicate with $p_{t,h}$ the h -th component of p_t , and Eq. (5) converts it into the binary decision $y_{t,h}$. We implemented each decision $y_{t,h}$ to be the outcome of a thresholding operation on $p_{t,h}$, so that

$$y_{t,h} = \begin{cases} 1, & \text{if } p_{t,h} \geq \gamma_h \\ 0, & \text{otherwise} \end{cases}$$

where $\gamma_h \in (0, 1)$ is the threshold associated to the h -th event.

We are given a training set composed of fully labeled video clips, so that we have a ground truth label $\hat{Y}_t = \{\hat{y}_{t,h}, h = 1, \dots, |\mathcal{E}|\}$ on each frame. For each sequence, the time index t spans from 1 to the length of the sequence itself, and we set s_0 to be a vector of zeros. We trained our network by computing a loss

function that, at each time instant, consists of the cross-entropy between the event-related output values and the ground truth,

$$\mathcal{L}_t = \sum_{h=1}^{|\mathcal{E}|} \{w_h \cdot [-\hat{y}_{t,h} \cdot \log(p_{t,h})] - (1 - \hat{y}_{t,h}) \cdot \log(1 - p_{t,h})\} .$$

Notice that we introduced the scalar $w_h > 0$ to weigh the contribute of the positive examples of class h . As a matter of fact, it is crucial to give larger weight to those events that are rarely represented in the training data, and our experience with the data of Section 3 suggests that an even weighing scheme frequently leads to not promising results (we choose $w_1 = 10$, $w_2 = 40$, $w_3 = 30$, $w_4 = 100$, following the event ordering of Section 2).

We evaluated four different deep networks that follow the aforementioned computations, and that are depicted in Fig. 5, together with several numerical details. The networks differ in the frame representation r_t that they process (Eq. (1)) and in the way they implement the **feature_extraction** function of Eq. (2). The first network, referred to as *hist*, processes the histogram of the motion features in the input frame, that are fed to the RNN without further processing ($q_t = r_t$). The second network, *conv*, is based on the appearance-only representation of each frame, i.e. $r_t = \text{gray}(\mathcal{I}_t)$, and it extracts features using a Convolutional Neural Network (CNN) with 3 layers (we also tested configurations with 2 layers). When the frame representation consists of the appearance $\text{gray}(\mathcal{I}_t)$ paired with the motion field (v_x, v_y) , then *conv* becomes the *convFlow* network. Finally, we also considered the effects of transfer learning in the *convPre* model, where we modified the *conv* net by plugging a pre-trained VGG-19 convolutional network [11] in Eq. (2). VGG-19 is composed of 19 layers and trained using the ImageNet database, so r_t is first rescaled/tiled to $224 \times 224 \times 3$ to match the size of the ImageNet data.

5 Experimental Results

We divided our dataset sets of video clips into three groups for fitting, validating and testing our models, with a ratio of 70%, 20%, 10%, keeping the original distribution of events in each split. We selected the F1 measure to evaluate the models of Section 4, and since some events occur very rarely in the data (see Section 3), we computed the F1 for each single event class. In particular, for every tested architecture, we selected the optimal value of the decision threshold γ_h ensuring the best performances on the validation set (testing multiple values in $[0.1, 0.9]$). We trained our networks with stochastic gradient-based updates that occur after having processed each video clip, and we used the Adam optimizer with a learning rate of $3 \cdot 10^{-5}$, processing the training data for 350 epochs. The training times are reported in Tab. 2, considering a system equipped with an Nvidia GTX Titan GPU (recall that the CNN of *convPre* is pre-trained).

We summarize the best performances obtained, for each class of event, by the *hist*, *conv*, *convFlow*, *convPre* models of Fig. 5 with multiple layers or recurrence.

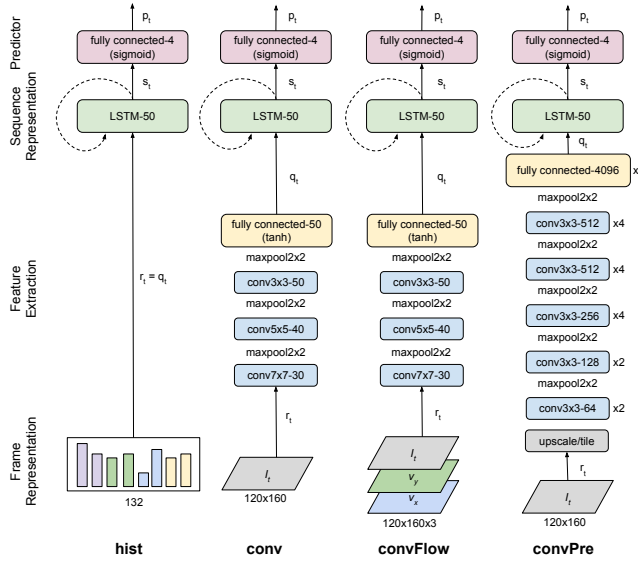


Fig. 5: Deep architectures applied to our task. Layer names are followed by the suffix $-n$, where n is the number of output units (or the size of the hidden state in LSTM). We use the ReLu activation, unless differently indicated in brackets. In convolutional and pooling layers we report the size of their spatial coverage (e.g., $k \times k$). In Section 5 we evaluate several variants of these nets.

Table 2: Avg training times (hours). Frame representations were precomputed.

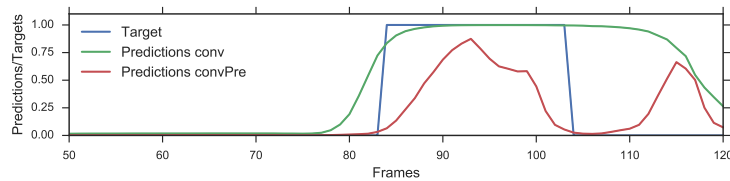
	hist	conv	convFlow	convPre
1 Layer RNN	2.03	15.12	17.05	3.91
2 Layers RNN	3.06	21.96	22.44	6.41

Depending on the model, we also evaluated different sizes of the recurrent state dimension h (20, 50, 132 for *hist*, 30, 50, 200 for *convPre*), or number of convolutional layers ℓ (2 or 3 layers for both *conv* and *convFlow*). These results show that the *hist* approach generally performs worse than the other models, and that convolutional architectures are a better solution to the proposed task, by virtue of their capability to extract autonomously relevant representation from images. When using 2 layers of RNNs, the configuration of *hist* with $h = 132$ leads to more competitive results, that, however, are paired with a larger computational burden than the CNN-based models due to the cost of computing its hand-engineered features. The *conv* model with only two convolutional layers shows good results paired with a computational cost that can be tolerated in real-time applications. The addition of the motion related information (*convFlow*) does not seem to help the performances. This can be explained by the fact that an architecture composed by a combination of a CNN together with a RNN is able

Table 3: Performances (F1) of the compared models.

		hist			conv		convFlow		convPre		
		$h = 20$	50	132	$\ell = 2$	3	$\ell = 2$	3	$h = 30$	50	200
(stationary)	1 Layer RNN	0.63	0.89	0.86	0.98	0.94	0.91	0.79	0.95	0.92	0.90
	2 Layers RNN	0.87	0.85	0.87	0.87	0.91	0.76	0.82	0.95	0.91	0.89
(departing)	1 Layer RNN	0.56	0.63	0.73	0.61	0.79	0.63	0.57	0.59	0.63	0.58
	2 Layers RNN	0.48	0.66	0.72	0.74	0.82	0.52	0.63	0.74	0.81	0.68
(wrong-way)	1 Layer RNN	0.59	0.84	0.89	0.92	0.93	0.89	0.92	0.96	0.93	0.94
	2 Layers RNN	0.83	0.87	0.89	0.86	0.88	0.86	0.88	0.94	0.93	0.91
(car crash)	1 Layer RNN	0.65	0.61	0.70	0.85	0.64	0.79	0.78	0.80	0.78	0.77
	2 Layers RNN	0.56	0.33	0.91	0.75	0.50	0.74	0.74	0.95	0.86	0.90
(average)	1 Layer RNN	0.61	0.74	0.80	0.84	0.83	0.81	0.77	0.83	0.82	0.80
	2 Layers RNN	0.69	0.68	0.85	0.81	0.78	0.72	0.77	0.90	0.88	0.85

by itself to grasp the temporal dynamics of a video, making an addition of optical flow features worthless. The use of a pre-trained network (*convPre*) leads to the best performances, on average, even if with a more costly inferential process. Finally, we notice that using 2 layers of RNNs does not add useful information to the *conv* model, while it always helps in *convPre*, mostly due to larger number of high-level features that are extracted by the CNN, where the system seems to find longer-term regularities (more easily captured by multiple layers of recurrence). The event class where all the models have shown worse performances is “departing”, that we explain by the larger incoherence in the training data in defining the beginning and, mostly, the ending frames of the event. In Fig. 6 we report an example that compares a prediction and the ground truth (test set), showing the mismatch in the ending-part of the event.

**Fig. 6:** Comparing predictions and ground truth in a “departing” event.

6 Conclusions

We described a deep-network-based implementation of an ATMS (Advanced Traffic Management System) that predicts a set of events while processing videos

of traffic on highways. We performed a detailed analysis of a real-world video data collection, investigating four classes of traffic events. We reported the results of an experimental evaluation that involved multiple representations of the input data and different deep architectures composed of a stack of convolutional and recurrent networks. Our results have shown that these networks can efficiently learn the temporal information from the video stream, simplifying the feature engineering process and making very promising predictions. We also proved the benefits of transferring the representations learned on a generic image classification task. Our best architectures will be tested online in real operative conditions.

References

1. Betsold, R.: Intelligent vehicle highway systems for the united states - an emerging national program. In: JSK International Symposium - Tech. Innovations for Tomorrow's Automobile Traffic and driving Information Systems. pp. 53 – 59 (1989)
2. Chen, C., Seff, A., Kornhauser, A., Xiao, J.: Deepdriving: Learning affordance for direct perception in autonomous driving. In: ICCV. pp. 2722–2730. IEEE (2015)
3. Coifman, B., Beymer, D., McLauchlan, P., Malik, J.: A real-time computer vision system for vehicle tracking and traffic surveillance. *Transportation Research Part C: Emerging Technologies* **6**(4), 271–288 (1998)
4. He, K., Zhang, X., Ren, S., Sun, J.: Deep residual learning for image recognition. In: *Proceedings of CVPR*. pp. 770–778 (2016)
5. Hochreiter, S., Schmidhuber, J.: Long short-term memory. *Neural computation* **9**(8), 1735–1780 (1997)
6. KaewTraKulPong, P., Bowden, R.: An improved adaptive background mixture model for real-time tracking with shadow detection. In: *Video-based surveillance systems*, pp. 135–144. Springer (2002)
7. Lee, W.H., Tseng, S.S., Shieh, W.Y.: Collaborative real-time traffic information generation and sharing framework for the intelligent transportation system. *Information Sciences* **180**(1), 62–70 (2010)
8. Michalopoulos, P.G., Fundakowski, R.A., Geokezas, M., Fitch, R.C.: Vehicle detection through image processing for traffic surveillance and control (Jul 11 1989), patent (US) 4,847,772
9. Oquab, M., Bottou, L., Laptev, I., Sivic, J.: Learning and transferring mid-level image representations using convolutional neural networks. In: *Proceedings of CVPR*. pp. 1717–1724. IEEE (2014)
10. Shibata, M.: Road traffic management in japan and development of the rac system. In: JSK International Symposium - Tech. Innovations for Tomorrow's Automobile Traffic and driving Information Systems. pp. 29 – 27 (1989)
11. Simonyan, K., Zisserman, A.: Very deep convolutional networks for large-scale image recognition. *arXiv preprint arXiv:1409.1556* (2014)
12. Williams, M.: Prometheus-european research programme for optimising the road transport system in europe. In: PROMETHEUS-The European research programme for optimising the road transport system in Europe. pp. 1–9 (Jan 1989)
13. Xu, D., Yan, Y., Ricci, E., Sebe, N.: Detecting anomalous events in videos by learning deep representations of appearance and motion. *Computer Vision and Image Understanding* **156**, 117 – 127 (2017). <https://doi.org/https://doi.org/10.1016/j.cviu.2016.10.010>